IDENTIFICATION OF COEXISTING ORTHO- AND CLINOPYROXENE BY ELECTRON BACKSCATTER DIFFRACTION IN CHEMICALLY HOMOGENOUS "ENSTATITE" GRAINS IN ALMAHATA SITTA UREILITES. Aidan J. Ross[1,2,3], Natasha R. Stephen[1] and Hilary Downes[2,3], [1]Plymouth Electron Microscopy Centre, University of Plymouth, UK., [2]Dept. of Earth Sciences, Natural History Museum, London, UK., [3]UCL/Birkbeck Joint Centre for Planetary Sciences, UCL, London, UK. (aidan.ross@ucl.ac.uk)

Introduction: Ureilites are ultramafic achondrites made up of olivine (ol), pyroxenes (px) and minor carbon, metal and sulfide accessory phases. Although olivine-pigeonite (ol-pig) assemblage is the most common, specimens featuring low-calcium pyroxene of nominally orthopyroxene (opx) composition (i.e., Wo ≤5) and/or augite (aug) are also found occurring with or without pigeonite e.g., [1, 2]. In the majority of ureilites exsolution of pyroxene is not evident. Silicate grains are generally chemically homogenous; other than the reverse zoning normally affecting the outermost grain rims caused by reduction, a ubiquitous and characteristic feature of ureilites, or mosaicized regions [1, 2]. Ol-pig and ol-opx samples are believed to represent restites of silicate partial melting and are believed to have the same origin despite different pyroxene compositions based on chemical similarities, such as falling along the same Fe/Mg-Fe/Mn trend [2].

The Almahata Sitta (AhS) fall of 2008 is comprised of clasts of a variety of meteorite types, although it is predominantly ureilitic [3, 4]. Zolensky *et al.* [3] conducted electron backscatter diffraction (EBSD) on the first studied specimen of AhS, which is an unusual fine-grained, highly porous lithology. They found opx grains with Ca contents as low as Wo=2 to have the monoclinic $P2_1/c$ space group, which they determined to be pigeonite rather than clinoenstatite based on the observation that "phases do not exhibit either kink banding, or consist of a fine mixture of lamellae of orthoenstatite and clinoenstatite, which are characteristic of low-temperature clinoenstatite" [3].

XRD and TEM observations of opx in some ureilites show complex ortho- and clinopyroxene (cpx) structures at the nm scale, some of which has been attributed to shock [e.g. 5]. Mittlefehldt *et al.* [1] hypothesized that all grains with nominally opx composition were originally protoenstatite.

In this work we applied multiple techniques to two ol-opx-pig AhS specimens to determine px type.

Methods: Distributions of minerals were calculated by combining X-ray maps collected on a LEO 1455 VP SEM at the Natural History Museum (NHM) and determining phase area percentages in Photoshop. Chemical compositions were determined using the Cameca SX100 electron microprobe at the NHM. Electron Backscatter Diffraction (EBSD) analysis was conducted at the University of Plymouth using a JEOL 6610 LV SEM with Oxford Instruments NordlysNano EBSD detector and AZtec software. Data reduction was performed using CHANNEL 5 and AZtec Crystal. Step sizes of 9-12 μm were used. Reference structures of enstatite (Pbca space group) [6] and pigeonite ($P2_1/c$ space group) [7] were used for indexing. This particular pigeonite reference structure was chosen because it is very similar in Ca content to the opx grains found here. Clinoenstatite has the same space group as pigeonite and they are therefore impossible to distinguish using EBSD methods alone.

Results: We studied pyroxenes in two ol-opx-pig specimens: AhS #22 (Fo=80.4) and AhS #36 (Fo=90.4). Both samples show low to medium shock, i.e., olivines are not mosaicized. Other optical indicators of shock could not be determined.

EPMA chemical compositions: Using the scheme of [8], the lower Ca pyroxene is enstatite and the higher Ca pyroxene is pigeonite in both samples. Multiple random points were analyzed in each pyroxene grain with very little difference being found within or between grains in each sample. These grains appear homogenous in backscattered electron images, excluding some small areas of possible melt infiltration of pigeonite in AhS #22. AhS #22 is previously unstudied by other authors, AhS #36 compositions agree with [3].

Table 1: Pyroxene compositions in different samples. n equals the total number of analyses across all grains.

Sample	Enstatite Wo//En	Pigeonite Wo/En
AhS #22	4.76/78.9 (n=23)	9.46/74.0 (n=9)
AhS #36	4.99/86.6 (n=57)	9.24/82.3 (n=13)

Modal mineralogies: Both AhS #22 and AhS #36 are ol-dominated but also contain two varieties of low-Ca pyroxene. We preliminarily label these as opx and pig based on their chemistries only.

Table 2: Silicate modalities. *px=px/(ol+px)

Sample	Ol %	Opx %	Pig %	*px
AhS #22	72	14	14	0.28
AhS #36	60	36	4	0.40

EBSD mapping: Up until this point, we have described pyroxenes solely by their chemical composition. EBSD, however, allows for examination of the crystallographic state of the pyroxenes at a μm scale, including mapping spatial distribution of different

phases. Using EBSD, we find that in both AhS #22 and AhS #36, the "enstatite" grains are made up of a combination of subgrains of ortho- and clinopyroxene structures, matching referenced enstatite [6] and pigeonite [7] (see Fig 1.).

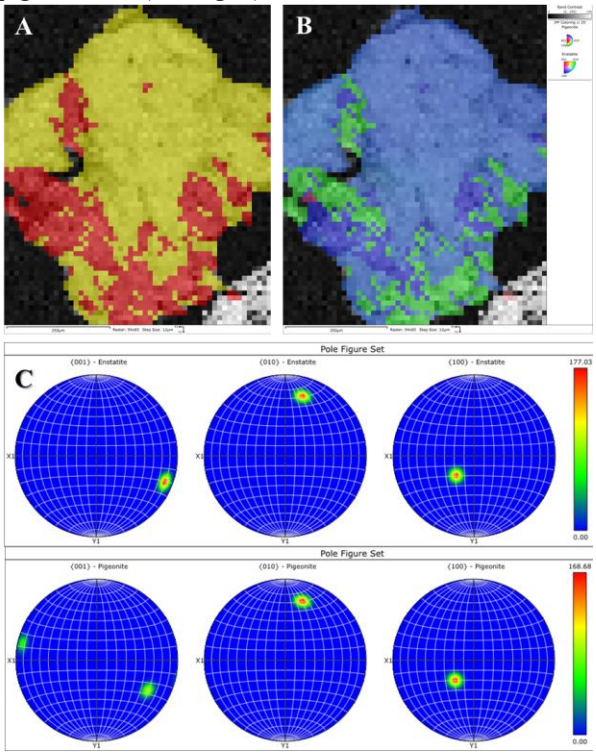

Fig 1: (A) Structural phase map of a single compositionally "enstatite" grain. Red = pigeonite, yellow = enstatite, white = olivine **(B)** IPF Map showing relative orientations of different phases within the grain **(C)** Pole figure showing orientations of axes for all points classified as enstatite (top) and pigeonite (bottom); both plots use 10 ° half-width, with max MUD values of 177 and 169 respectively. Clustering indicates a single orientation, except in pigeonite {001} where two orientations are observed.

Both AhS #22 and AhS #36 show that the enstatite and pigeonite subgrains are discontinuous in places (Fig. 1(A)). They do not appear to be twinned. Shock is also an unlikely cause for the two different structures internal strain is minimal; little variance in color within subgrains in IPF maps is observed (Fig. 1(B)), implying minimal misorientation. This is confirmed with the clustered axis locations in both pole figures (Fig 1(C)).

Comparison of orientations of the subgrains shows a very close match in {010} between pigeonite and enstatite subgrains in all cases, and a fairly close match in {100}, whereas there is a deviation in orientations along {001} (Figs. 1(C)). This is true in all the grains analyzed. In AhS #36, the pigeonite subgrains were found to have two orientations along {001} within a single whole grain, as seen in Fig. 1(C).

Compositionally pigeonite whole grains mapped by EBSD were found to be only single crystals of pigeonite structure without any internal features of interest, (see Fig. 2).

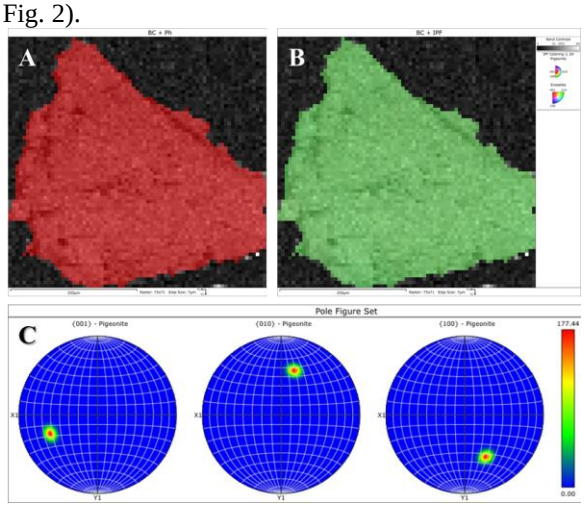

Fig 2: (A) Crystallographic phase map of a single compositionally pigeonite grain. Red = pigeonite, **(B)** IPF Map showing relative orientations observed within the grain, with only one orientation identifiable **(C)** Pole figure showing orientations for all points mapped in A + B (pigeonite); The plot uses a 10 ° half-width, with max MUD values of 177 Clustering indicates a single orientation along all planes {001}, {010}, {100}.

Implications: Although the findings of [3] make the argument that all low-Ca pyroxenes should be referred to as such, they studied a highly shocked sample that may have precipitated a change in structure. Our findings suggest that larger, lower shock, chemically-defined enstatites are made up of both ortho- and clino-structures, (namely enstatite, and then pigeonite or clinoenstatite). Grains chemically-defined as pigeonite appear crystallographically to be single grains. Therefore, this study confirms that the common classification scheme of ol-pig and ol-opx ureilites is correct and should be used in ureilite classification.

Acknowledgements: We would like to thank John Spratt for assistance with the EPMA and Alex Ball for assistance with the SEM at the NHM.

References: [1] Mittlefehldt D. W. *et al.* (1998) *RiM*, Ch. 4. [2] Goodrich C. A. *et al.* (2004) *Chemie der Erde 64*: 283-327. [3] Zolensky *et al.* (2010) *Meteoritics & Planet. Sci. 45*: 1618-1637. [4] Bischoff *et al.* (2010) *Meteoritics & Planet. Sci. 45*: 1638-1656. [5] Takeda H. (1989) *Earth Planet Sci Lett 93*: 181-194. [6] Yang H. and Ghose S. (1995) *Am. Min 80*:9-20 [7] Morimoto N. and Güven N. (1970) *Am. Min. 55*: 1195-1209. [8] Morimoto N. *et al.* (1988) *Am. Min. 73*: 1123-1133.